Chapter 24

Three Types of Fuzzy Controllers Applied in High-Performance Electric Drives for Three-Phase Induction Motors

José Luis Azcue, Alfeu J. Sguarezi Filho and Ernesto Ruppert

Additional information is available at the end of the chapter

http://dx.doi.org/10.5772/48388

1. Introduction

The electric drives are very common in industrial applications because they provide high dynamic performance. Nowadays exist a wide variety of schemes to control the speed, the electromagnetic torque and stator flux of three-phase induction motors. However, control remains a challenging problem for industrial applications of high dynamic performance, because the induction motors exhibit significant nonlinearities. Moreover, many of the parameters vary with the operating conditions. Although the Field Oriented Control (FOC) [16] schemes are attractive, but suffer from a major disadvantage, because they are sensitive to motor parameter variations such as the rotor time constant, and an incorrect flux estimation at low speeds. Another popular scheme for electric drives is the direct torque control (DTC) scheme [15][8], and an another DTC scheme based on space vector modulation (SVM) technique that reduces the torque ripples. This scheme does not need current regulators because its control variables are the electromagnetic torque and the stator flux. In this chapter we use the DTC-SVM scheme to analyze the performance of our proposed fuzzy controllers.

In the last decade, there was an increasing interest in combining artificial intelligent control tools with conventional control techniques. The principal motivations for such a hybrid implementation were that fuzzy logic issues such as uncertainty (or unknown variations in plant parameters and structure) can be dealt with more effectively. Hence improving the robustness of the control system. Conventional controls are very stable and allow various design objectives such as steady state and transient characteristics of a closed loop system. Several [5][6] works contributed to the design of such hybrid control schemes.

However, fuzzy controllers, unlike conventional PI controllers do not necessarily require the accurate mathematic model of the process to be controlled; instead, it uses the experience and knowledge about the controlled process to construct the fuzzy rules base. The fuzzy logic

controllers are a good alternative for motor control systems since they are well known for treating with uncertainties and imprecisionï£¡'s. For example, in [1] the PI and fuzzy logic controllers are used to control the load angle, which simplifies the induction motor drive system. In [7], the fuzzy controllers are used to dynamically obtain the reference voltage vector in terms of torque error, stator flux error and stator flux angle. In this case, both torque and stator flux ripples are remarkably reduced. In [10], the fuzzy PI speed controller has a better response for a wide range of motor speed and in [3] a fuzzy self-tuning controller is implemented in order to substitute the unique PI controller, present in the DTC-SVM scheme. In this case, performance measures such as settling time, rise time and ITAE index are lower than the DTC-SVM scheme with PI controller.

The fuzzy inference system can be used to modulate the stator voltage vector applied to the induction motor [18]. In this case, unlike the cases mentioned above, the quantity of available vectors are arbitrarily increased, allowing better performance of the control scheme and lower levels of ripple than the classic DTC. However, it requires the stator current as an additional input, increasing the number of input variables. In this chapter we design and analyze in details three kinds of fuzzy controllers: the PI fuzzy controller (PI-F), the PI-type fuzzy controller (PIF) and the self-tuning PI-type fuzzy controller (STPIF). All of these fuzzy controllers are applied to a direct torque control scheme with space vector modulation technique for three-phase induction motor. In this DTC-SVM scheme, the fuzzy controllers generate corrective control actions based on the real torque trend only while minimizing the torque error.

2. Background

2.1. The three-phase induction motor dynamical equations

By the definitions of the fluxes, currents and voltages space vectors, the dynamical equations of the three-phase induction motor in stationary reference frame can be put into the following mathematical form [17]:

$$\vec{u}_s = R_s\vec{i}_s + \frac{d\vec{\psi}_s}{dt} \tag{1}$$

$$0 = R_r\vec{i}_r + \frac{d\vec{\psi}_r}{dt} - j\omega_r\vec{\psi}_r \tag{2}$$

$$\vec{\psi}_s = L_s\vec{i}_s + L_m\vec{i}_r \tag{3}$$

$$\vec{\psi}_r = L_r\vec{i}_r + L_m\vec{i}_s \tag{4}$$

Where $\vec{u}_s$ is the stator voltage space vector, $\vec{i}_s$ and $\vec{i}_r$ are the stator and rotor current space vectors, respectively, $\vec{\psi}_s$ and $\vec{\psi}_r$ are the stator and rotor flux space vectors, ω_r is the rotor angular speed, R_s and R_r are the stator and rotor resistances, L_s, L_r and L_m are the stator, rotor and mutual inductance respectively.

The electromagnetic torque t_e is expressed in terms of the cross-vectorial product of the stator and the rotor flux space vectors.

$$t_e = \frac{3}{2}P\frac{L_m}{L_rL_s\sigma}\vec{\psi}_r \times \vec{\psi}_s \tag{5}$$

$$t_e = \frac{3}{2}P\frac{L_m}{L_rL_s\sigma}\left|\vec{\psi}_r\right|\left|\vec{\psi}_s\right|\sin(\gamma) \tag{6}$$

Where γ is the load angle between stator and rotor flux space vector, P is a number of pole pairs and $\sigma = 1 - L_m^2/(L_s L_r)$ is the dispersion factor.

The three-phase induction motor model was implemented in MATLAB/Simulink as is shown in [2].

2.2. The principle of direct torque control

In the direct torque control if the sample time is short enough, such that the stator voltage space vector is imposed to the motor keeping the stator flux constant at the reference value. The rotor flux will become constant because it changes slower than the stator flux. The electromagnetic torque (6) can be quickly changed by changing the angle γ in the desired direction. This angle γ can be easily changed when choosing the appropriate stator voltage space vector.

For simplicity, let us assume that the stator phase ohmic drop could be neglected in (1). Therefore $d\vec{\psi}_s/dt = \vec{u}_s$. During a short time Δt, when the voltage space vector is applied it has:

$$\Delta\vec{\psi}_s \approx \vec{u}_s \cdot \Delta t \tag{7}$$

Thus the stator flux space vector moves by $\Delta\vec{\psi}_s$ in the direction of the stator voltage space vector at a speed which is proportional to the magnitude of the stator voltage space vector. By selecting step-by-step the appropriate stator voltage vector, it is possible to change the stator flux in the required direction.

3. Direct torque control scheme with space vector modulation technique

In Fig. 1, we show the block diagram for the DTC-SVM scheme [14] with a Fuzzy Controller, the fuzzy controller will be substitute for the three kind of proposed Fuzzy Controller one for time. The DTC-SVM scheme is an alternative to the classical DTC schemes [15], [8] and [9]. In this one, the load angle γ^* is not prefixed but it is determinate by the Fuzzy Controller. Equation (6) shows that the angle γ^* determines the electromagnetic torque which is necessary to supply the load. The three proposed Fuzzy Controllers determine the load angle using the torque error e and the torque error change Δe. Details about these controllers will be presented in the next section. Figure 1 shows the general block diagram of the DTC-SVM scheme, the inverter, the control signals for three-phase two-level inverter is generated by the DTC-SVM scheme.

3.1. Flux reference calculation

In stationary reference frame, the stator flux reference $\vec{\psi}_s^*$ can be decomposed in two perpendicular components ψ_{ds}^* and ψ_{qs}^*. Therefore, the output of the fuzzy controller γ^* is added to rotor flux angle $\angle\vec{\psi}_r$ in order to estimate the next angle of the stator flux reference.

In this chapter we consider the magnitude of stator flux reference as a constant. Therefore, we can use the relation presented in equation (8) to calculate the stator flux reference vector.

$$\vec{\psi}_s^* = |\vec{\psi}_s^*|\cos(\gamma^* + \angle\vec{\psi}_r) + j|\vec{\psi}_s^*|\sin(\gamma^* + \angle\vec{\psi}_r) \tag{8}$$

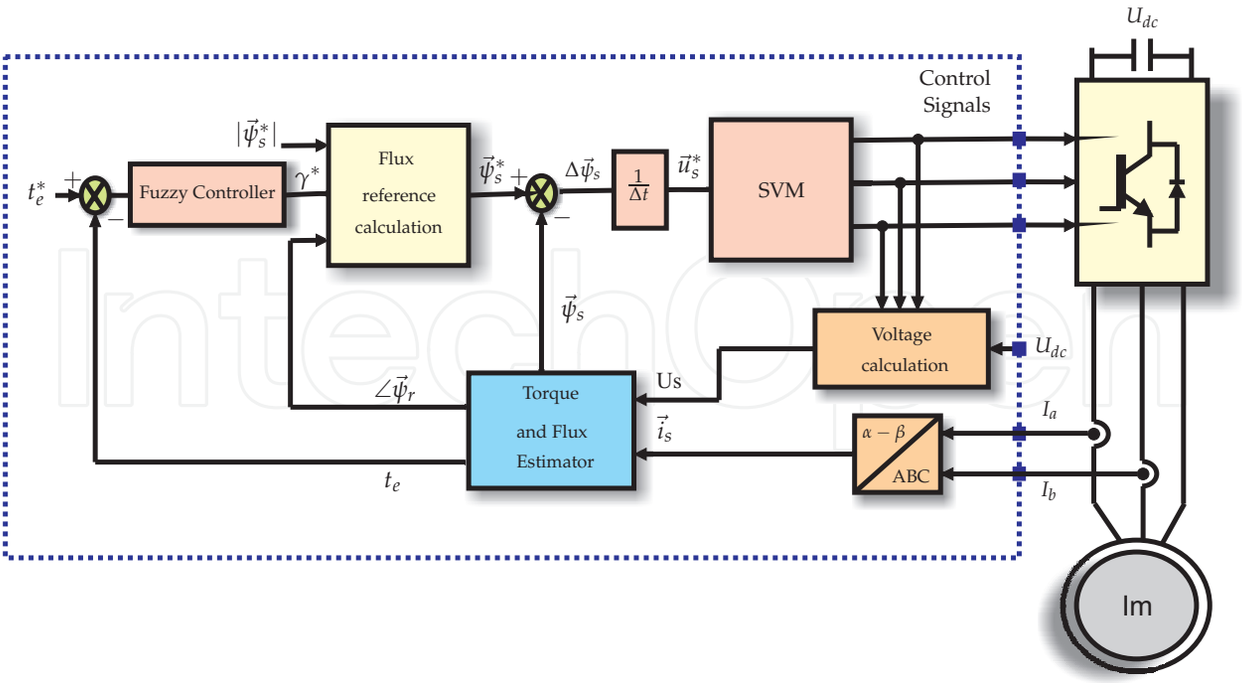

Figure 1. Direct torque control with space vector modulation scheme and fuzzy controller.

Moreover, if we consider the stator voltage $\vec{u}_s$ during a short time Δt, it is possible to reproduce a flux variation $\Delta\vec{\psi}_s$. Notice that the stator flux variation is nearly proportional to the stator voltage space vector as seen in the equation (7).

3.2. Stator voltage calculation

The stator voltage calculation uses the DC link voltage (U_{dc}) and the inverter switch state (S_{Wa}, S_{Wb}, S_{Wc}) of the three-phase two level inverter. The stator voltage vector $\vec{u}_s$ is determined as in [4]:

$$\vec{u}_s = \frac{2}{3}\left[(S_{Wa} - \frac{S_{Wb}+S_{Wc}}{2}) + j\frac{\sqrt{3}}{2}(S_{Wb}-S_{Wc})\right]U_{dc} \tag{9}$$

3.3. Electromagnetic torque and stator flux estimation

As drawn by Fig. 1 the electromagnetic torque and the stator flux estimation depend on the stator voltage and the stator current space vectors,

$$\vec{\psi}_s = \int(\vec{u}_s - R_s\cdot\vec{i}_s)dt \tag{10}$$

The problem with this kind of estimation is that for low speeds the back electromotive force (emf) depends strongly of the stator resistance, to resolve this problem is used the current model to improve the flux estimation as in [13]. The rotor flux $\vec{\psi}_{rdq}$ represented in the rotor flux reference frame is given by:

$$\vec{\psi}_{rdq} = \frac{L_m}{1+sT_r}\vec{i}_{sdq} - j\frac{(\omega_{\psi_r}-\omega_r)T_r}{1+sT_r}\vec{\psi}_{rdq} \tag{11}$$

Notice that $T_r = L_r/R_r$ is the rotor time constant, and $\psi_{rq} = 0$. Substituting this expression in the equation (11) yields:

$$\psi_{rd} = \frac{L_m}{1 + sT_r} i_{sd} \tag{12}$$

In the current model the stator flux is represented by:

$$\vec{\psi}_s^i = \frac{L_m}{L_r}\vec{\psi}_r^i + \frac{L_s L_r - L_m^2}{L_r}\vec{i}_s \tag{13}$$

Where $\vec{\psi}_r^i$ is the rotor flux according to the equation (12). Since the voltage model is based on equation (1), the stator flux in the stationary reference frame is given by

$$\vec{\psi}_s = \frac{1}{s}(\vec{v}_s - R_s\vec{i}_s - \vec{U}_{comp}) \tag{14}$$

With the aim to correct the errors associated with the pure integration and the stator resistance measurement, the voltage model is adapted through the PI controller.

$$\vec{U}_{comp} = (K_p + K_i\frac{1}{s})(\vec{\psi}_s - \vec{\psi}_s^i) \tag{15}$$

The K_p and K_i coefficients are calculated with the recommendation proposed in [13]. The rotor flux $\vec{\psi}_r$ in the stationary reference frame is calculated as:

$$\vec{\psi}_r = \frac{L_r}{L_m}\vec{\psi}_s - \frac{L_s L_r - L_m^2}{L_m}\vec{i}_s \tag{16}$$

The estimator scheme shown in the Fig. 2 works with a good performance in the wide range of speeds.

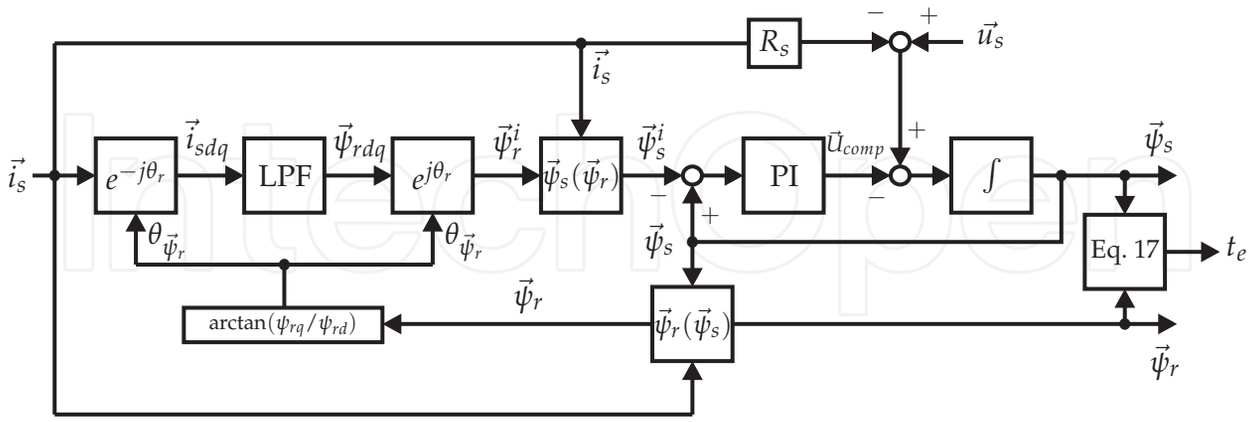

Figure 2. Stator and rotor flux estimator, and electromagnetic torque estimator.

Where LPF means low pass filter. In the other hand, when equations (14) and (16) are replaced in (5) we can estimated the electromagnetic torque t_e as:

$$t_e = \frac{3}{2}P\frac{L_m}{L_r L_s \sigma}\vec{\psi}_r \times \vec{\psi}_s \tag{17}$$

4. Design of fuzzy controllers

4.1. The PI fuzzy controller (PI-F)

The PI fuzzy controller combines two simple fuzzy controllers and a conventional PI controller. Note that fuzzy controllers are responsible for generating the PI parameters dynamically while considering only the torque error variations. The PI-F block diagram is shown in Fig. 3, this controller is composed of two scale factors G_e, $G_{\Delta e}$ at the input. The input for fuzzy controllers are the error (e_N) and error change ($e_{\Delta N}$), and theirs outputs represent the proportional gain K_p and the integral time T_i respectively. These parameters K_p and T_i are adjusted in real time by the fuzzy controllers. The gain K_P is limited to the interval $[K_{p,min}, K_{p,max}]$, which we determined by simulations. For convenience, K_P is normalized in the range between zero and one through the following linear transformation.

$$K_p^{'} = \frac{K_p - K_{p,min}}{K_{p,max} - K_{p,min}} \tag{18}$$

Then, considering that the fuzzy controller output is a normalized value $K_p^{'}$, we obtain K_p by:

$$K_p = (K_{p,min} - K_{p,max})K_p^{'} + K_{p,min} \tag{19}$$

However, for different reference values the range for the proportional gain values is chosen as $[0, K_{p,max}]$,

$$K_p = K_{p,max}K_p^{'} \tag{20}$$

Due to nonlinearities of the system and in order to avoid overshoots for large reference torque r, it is necessary to reduce the proportional gain. We use a gain coefficient $\rho = 1/(1 + 0002 * r)$ that depends on the reference values. In order to achieves real time adjustment for the K_p values. Therefore, $K_{p,max} = \rho K_{p,max0}$ where the value $K_{p,max0} = 1.24$ was obtained through various simulations. Note that both ρ and $K_{p,max}$ decreases as the reference value increases. Consequently, the gain K_p decreases. The PI-F controller receives as input the torque error e and as output the motor load angle γ^*.

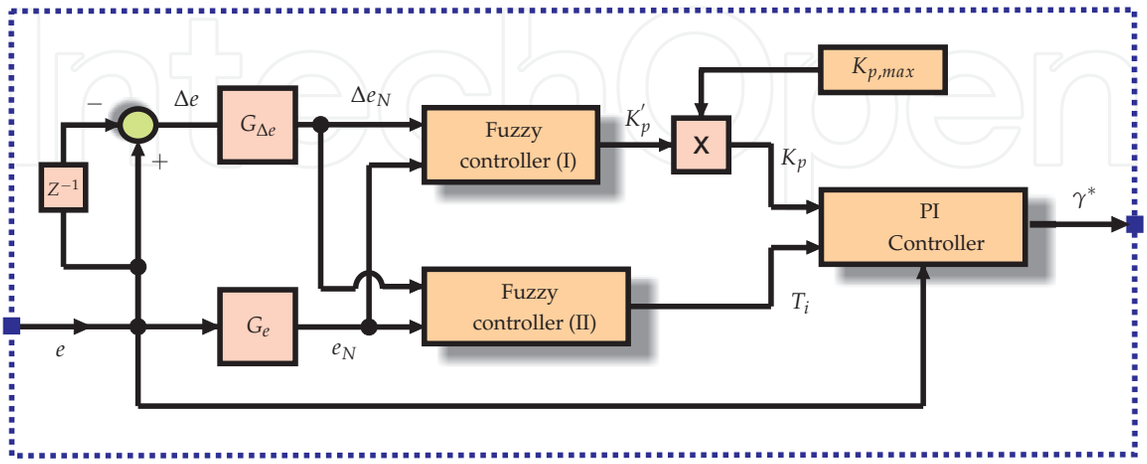

Figure 3. PI Fuzzy Controller block diagram.

4.1.1. Membership Functions (MF)

In the Fig. 3, the first fuzzy controller receives as inputs the errors $e_N, \Delta e_N$, each of them has three fuzzy sets that are defined similarly, being only necessary to describe the fuzzy sets of the first input. The first input e_N has three fuzzy sets whose linguistic terms are N-Negative, ZE-Zero and P-Positive. Each fuzzy set has a membership function associated with it. In our particular case of, these fuzzy sets have trapezoidal and triangular shapes as shown in Fig.4. The universe of discourse of these sets is defined over the closed interval $[-1.5, 1.5]$.

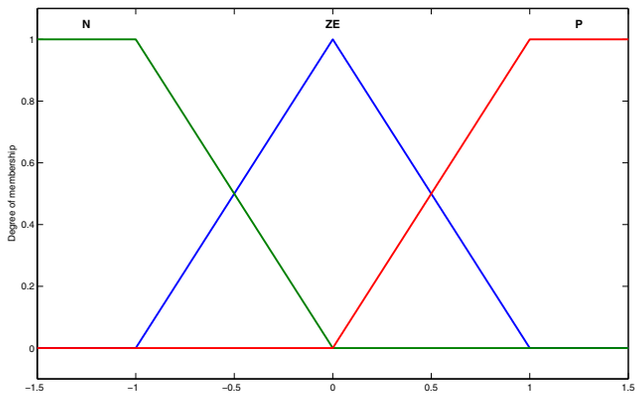

Figure 4. Membership functions for the inputs e_N, Δe_N.

The output has two fuzzy sets whose linguistic values are associated with them are S-small and B-Big, respectively. Both have trapezoidal membership functions as shown in Fig.5. The universe of discourse of the fuzzy sets is defined over the closed interval $[-0.5, 1.5]$. The fuzzy controller uses: triangular norm, Mamdani implication, max-min aggregation method and the center of mass method for defuzzification [11].

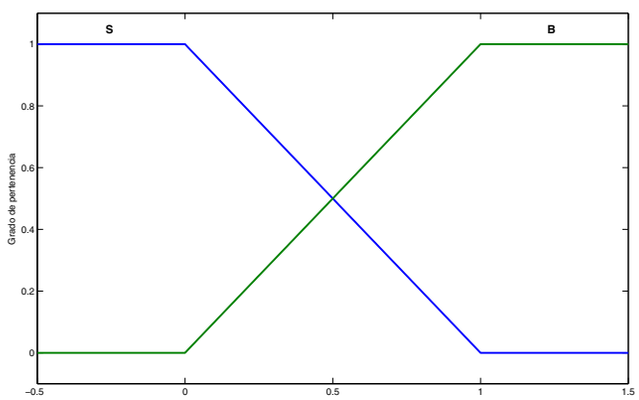

Figure 5. Membership functions for the first fuzzy controller output K_p.

Similarly, the second fuzzy controller has the same fuzzy sets for its two inputs, however, its output is defined by three constant values defined as 1.5, 2 and 3 which linguistic values associated with them are S-Small, M-Medium and B-Big. This controller uses the zero-order Takagi-Sugeno model which simplifies the hardware design and is easy to

introduce programmability [19]. The defuzzification method used for this controller is the weighted sum.

4.1.2. Scaling Factors (SF)

The PI-F controller has two scaling factors, G_e and $G_{\Delta e}$ as inputs, while the fuzzy controllers outputs are the gain $K_p^{'}$ and the integral time T_I respectively. From these values we can calculate the parameter $K_I = K_p / T_I$.

The scale factor ensures that both inputs are within the universe of discourse previously defined. The parameters K_p and K_I are the tuned parameters of the PI controller. The inputs are normalized, by:

$$e_N = G_e \cdot e \tag{21}$$

$$\Delta e_N = G_{\Delta e} \cdot \Delta e \tag{22}$$

4.1.3. The rule bases

The rules are based on simulation that we conducted of various control schemes. Fig.6 shows an example for one possible response system. Initially, the error is positive around the point *a*, and the error change is negative, then is imposed a large control signal in order to obtain a small rise time.

To produce a large signal control, the PI controller should have a large gain K_p and a large integral gain K_I (small integral time T_I), therefore,

$$R_x: \text{ if } e_N \text{ is } S \text{ and } \Delta e_N \text{ is } N \text{ then } K_p \text{ is } G$$

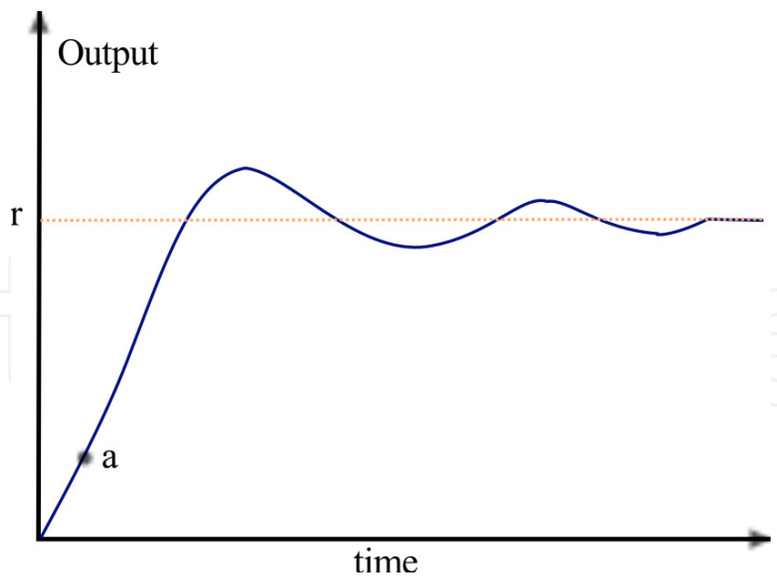

Figure 6. Response system.

The rule base for the first fuzzy controller is in Table 1, also, the rule base for the second fuzzy controller is in Table 2.

Fig. 7 shows the control surface for the first and second fuzzy controllers. This figure clearly shows the non-linear relationship between (e, Δe, K_p) and (e, Δe, T_I)

e_N / Δe_N	N	ZE	P
N	B	B	B
ZE	S	B	S
P	B	B	B

Table 1. Rule base for fuzzy controller (I), output K'_p

e_N / Δe_N	N	ZE	P
N	S	S	S
ZE	B	M	B
P	S	S	S

Table 2. Rule base for fuzzy controller (II), output T_I

4.2. The PI-type fuzzy controller (PIF) and The self-tuning PI-type fuzzy controller (STPIF)

The PI-type fuzzy controller (PIF) is a fuzzy controller inspired by a digital PI controller, which is depicted in Fig. 8. It is composed by two input scale factors "G_e, $G_{\Delta e}$" and one output scale factor "G_{γ^*}". Finally it uses saturation block to limit the output.

This controller has a single input variable, which is the torque error "e" and one output variable which is the motor load angle "γ^*" given by:

$$\gamma^*(k) = \gamma^*(k+1) + \Delta\gamma^*(k) \tag{23}$$

In (23), k is the sampling time and $\Delta\gamma^*(k)$ represents the incremental change of the controller output. We wish to emphasize here that this accumulation (23) of the controller output takes place out of the fuzzy part of the controller and it does not influence the fuzzy rules.

Fig.9 shows the self-tuning PI-type fuzzy controller (STPIF) block diagram, its main difference with the PIF controller is the gain tuning fuzzy controller (GTF) block.

4.2.1. Membership Functions (MF)

The MF for PIF controller are shown in Fig. 10(a). This MF for input variables "e_N, Δe_N" and output variable "$\Delta\gamma_N^*$" are normalized in the closed interval [-1,1].

The MF's for GTF controller are shown in Fig. 10(a) and in Fig. 10(b) for input and output variables respectively. Input variables "e_N, Δe_N" are defined in the closed interval [-1,1] and the output variable "α" is defined in the closed interval [0,1].

Most of the MF variables have triangular shape [Fig. 10] with 50% overlapping neighbor functions, except the extremes which are trapezoidal. The linguistic variables are referred to as: NL-Negative Large, NM-Negative Medium, NS-Negative Small, ZE-Zero, VS-Very Small, S-Small, SL-Small Large and so on as shown in Table 3 and in Table 4.

4.2.2. Scaling factors

The two inputs SF "$G_{\Delta e}$, G_e" and the output SF "G_{γ^*}" can be adjusted dynamically through updating the scaling factor "α". "α" is computed on-line, using a independent fuzzy rule model

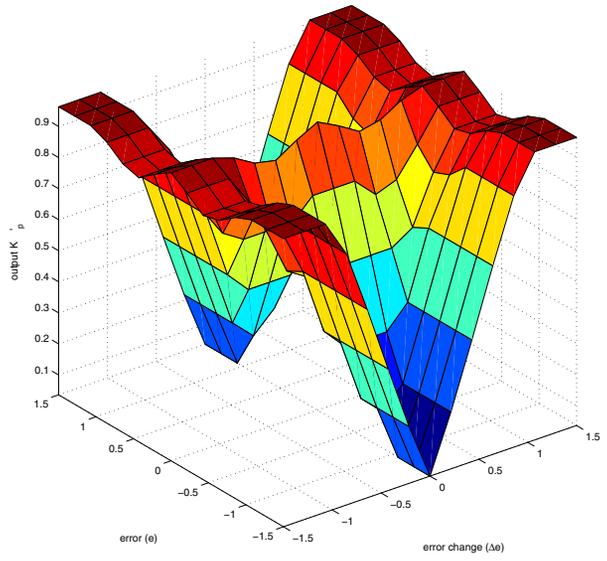

(a) Control surface for fuzzy controller (I), output $K_p^{'}$.

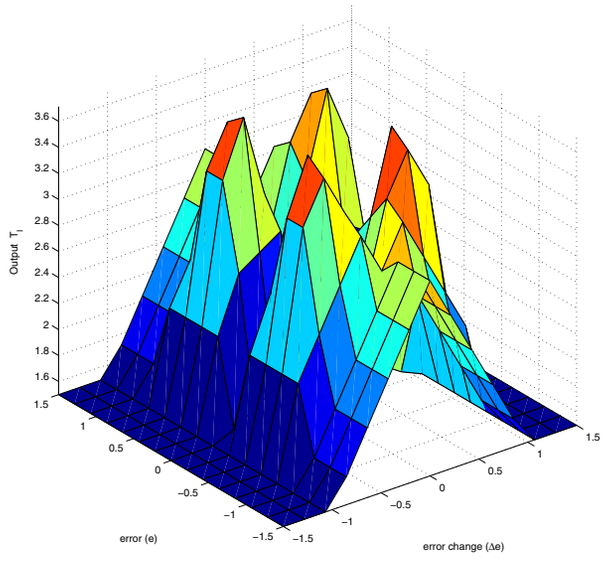

(b) Control surface for fuzzy controller (II), output T_I.

Figure 7. Control surface for: (a) fuzzy controller (I) and (b) fuzzy controller (II)

defined in terms of "e, Δe". The relationship between the SF and the input/output variables of the STPIF controller are shown bellow:

$$e_N = G_e \cdot e \tag{24}$$

$$\Delta e_N = G_{\Delta e} \cdot \Delta e \tag{25}$$

$$\Delta\gamma^* = (\alpha \cdot G_{\gamma^*}) \cdot \Delta\gamma_N^* \tag{26}$$

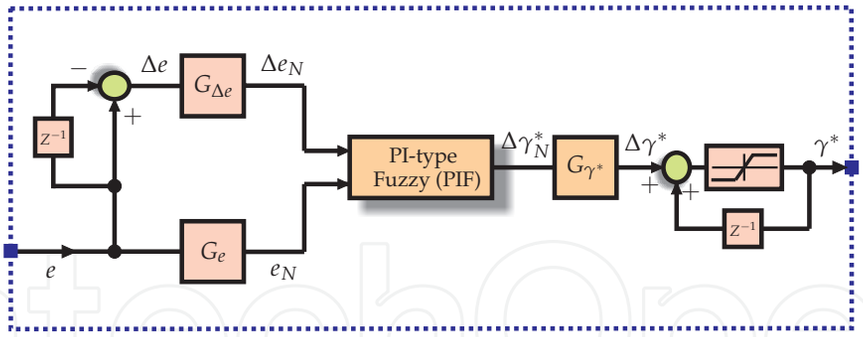

Figure 8. PI-type fuzzy controller.

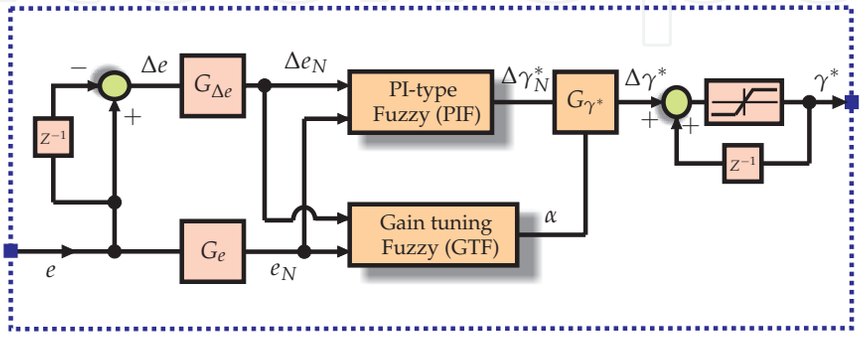

Figure 9. Self-tuning PI-type fuzzy (STPIF) controller.

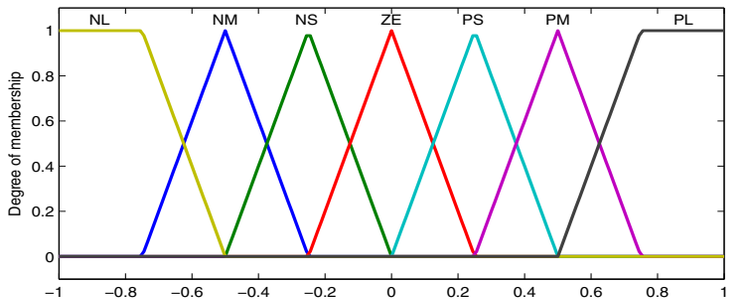

(a) Membership function for e_N, Δe_N and $\Delta\gamma_N^*$.

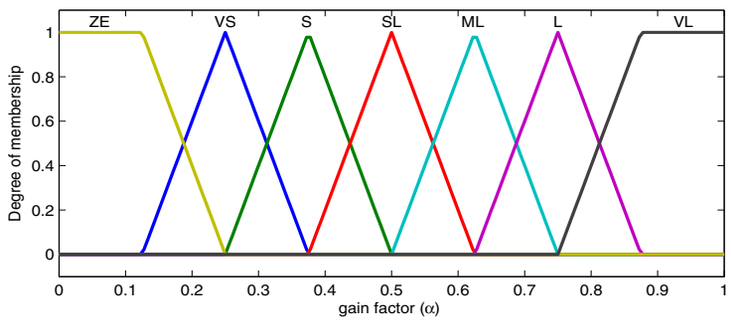

(b) Membership function for α for GTF controller output

Figure 10. Membership functions for: (a) error e_N and change of error Δe_N is the same for PIF and GTF controllers as well as for the output $\Delta\gamma_N^*$ of the PIF controller. (b) the gain updating factor α

4.2.3. The rule bases

The incremental change in the controller output $\Delta\gamma_N^*$ to PIF controller is defined as,

$$R_x: \text{ if } e_N \text{ is } E \text{ and } \Delta e_N \text{ is } \Delta E \text{ then } \Delta\gamma_N^* \text{ is } \Delta\Gamma_N^*$$

Where $E = \Delta E = \Delta\Gamma_N^* = \{NL, NM, NS, ZE, PS, PM, PL\}$. The output α of the GTF controller is determined by the following rules:

$$R_x: \text{ if } e_N \text{ is } E \text{ and } \Delta e_N \text{ is } \Delta E \text{ then } \alpha \text{ is } \chi$$

Where $E = \Delta E = \{NL, NM, NS, ZE, PS, PM, PL\}$ and $\chi = \{ZE, VS, S, SL, ML, L, VL\}$. The rule base for $\Delta\gamma_N^*$ and α are shown in Tab. 3 and Tab. 4 respectively.

Δe_N / e_N	NL	NM	NS	ZE	PS	PM	PL
NL	NL	NL	NL	NM	NS	NS	ZE
NM	NL	NM	NM	NM	NS	ZE	PS
NS	NL	NM	NS	NS	ZE	PS	PM
ZE	NL	NM	NS	ZE	PS	PM	PL
PS	NM	NS	ZE	PS	PS	PM	PL
PM	NS	ZE	PS	PM	PM	PM	PL
PL	ZE	PS	PS	PM	PL	PL	PL

Table 3. Fuzzy rules for the computation of $\Delta\gamma_N^*$

Δe_N / e_N	NL	NM	NS	ZE	PS	PM	PL
NL	VL	VL	VL	L	SL	S	ZE
NM	VL	VL	L	L	ML	S	VS
NS	VL	ML	L	VL	VS	S	VS
ZE	S	SL	ML	ZE	ML	SL	S
PS	VS	S	VS	VL	L	ML	VL
PM	VS	S	ML	L	L	VL	VL
PL	ZE	S	SL	L	VL	VL	VL

Table 4. Fuzzy rules for the computation of α

4.2.4. Gain tuning fuzzy

The purpose of the GTF controller is update continuous the value of α in every sample time. The output α is necessary to control the percentage of the output SF "G_{γ^*}", and therefore for calculating new "$\Delta\gamma^*$",

$$\Delta\gamma^* = (\alpha \cdot G_{\gamma^*}) \cdot \Delta\gamma_N^* \tag{27}$$

The GTF controller rule base is based on knowledge about the three-phase IM control, using a DTC type control according to the scheme proposed in [14], in order to avoid large overshoot and undershoot, e.g., when "e" and "Δe" have different signs, it means that the estimate torque

"t_e" is approaching to the torque reference "t_e^*", then the output SF "G_{γ^*}" must be reduced to a small value by "α", for instance, if "e" is "PM" and "Δe" is "NM" then "α" is "S".

On the other hand, when "e" and "Δe" have the same sign, it means that the torque estimate "t_e" is moving away from the torque reference "t_e^*", the output SF "G_{γ^*}" must be increased to a large value by "α" in order to avoid that the torque depart from the torque reference, e.g., if "e" is "PM" and "Δe" is "PM" then "α" is "VL".

The nonlinear relationship between "$e,\ \Delta e,\ \Delta\gamma_N^*$" and "$e,\ \Delta e,\ \alpha$" are shown in Fig. 11.

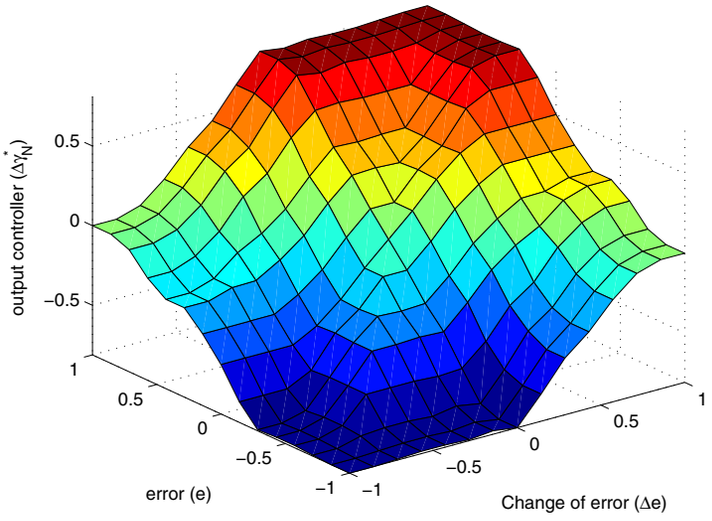

(a) Surface of PIF controller output ($\Delta\gamma_N^*$).

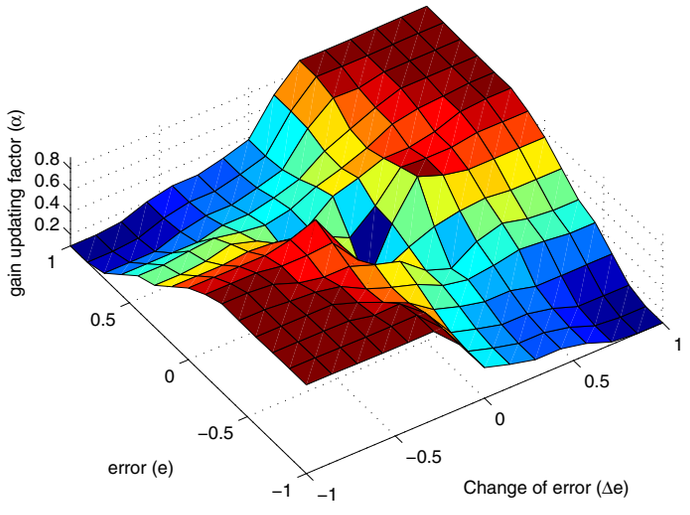

(b) Surface of GTF controller output (α).

Figure 11. Surface of: (a) PIF controller and (b) GTF controller

The inference method used in PIF and GTF controllers is the Mamdani's implication based on max-min aggregation. We use the center of area method for defuzzification.

5. Simulation results

We have conducted our simulation with MATLAB simulation package, which include Simulink block sets and fuzzy logic toolbox. The switching frequency of the pulse width modulation (PWM) inverter was set to be 10kHz, the stator reference flux considered was 0.47 Wb. In order to investigate the effectiveness of the three proposed fuzzy controllers applied in the DTC-SVM scheme we performed several tests.

We used different dynamic operating conditions such as: step change in the motor load (from 0 to 1.0 pu) at 90 percent of rated speed, no-load speed reversion (from 0.5 pu to -0.5 pu) and the application of a specific load torque profile at 90 percent of rated speed. The motor parameters used in the tests are given in Table 5.

Fig. 12, shows the response of the speed and electromagnetic torque when speed reversion for DTC-SVM with PI-F controller is applied. Here, the rotor speed changes its direction at about 1.8 seconds. Fig. 13 shows the stator and rotor current sinusoidal behavior when applying reversion.

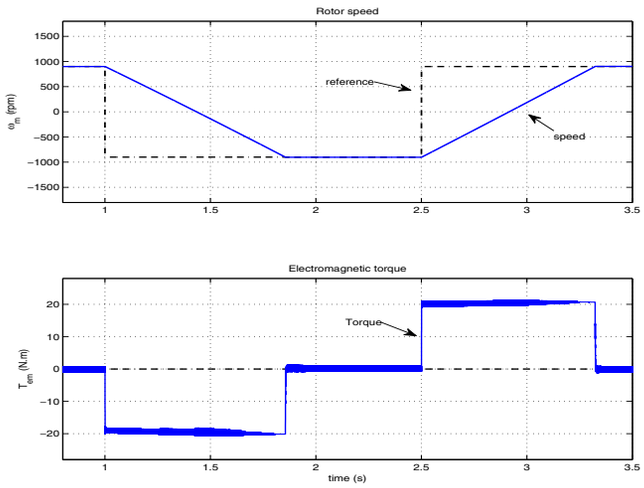

Figure 12. Speed reversion for DTC-SVM with PI-F controller.

Fig. 14 and Fig. 15 show the torque and currents responses respecively, when step change is applied in the motor load for DTC-SVM with the PI-F controller. This speed test was established at 90 percent of rated speed.

In Fig. 16, we demonstrate the speed response when applying a speed reversion for DTC-SVM with PIF controller. In this case the speed of the rotor changes its direction at about 1.4 seconds. Fig. 17 shows the electromagnetic torque behavior when the reversion is applied.

Fig. 18 and Fig. 19 show the response of the electromagnetic torque and phase *a* stator current respectively, when applying a step change in the motor load for DTC-SVM whit PIF controller. In this test the speed of the motor was set to 90 percent of rated speed.

Fig. 20 shows the behaviors of the electromagnetic torque, phase *a* stator current and the motor speed, when applying speed reversion from 0.5 pu to -0.5 pu in the DTC-SVM scheme with STPIF controller. The sinusoidal waveform of the current shows that this control technique also leads to a good current control.

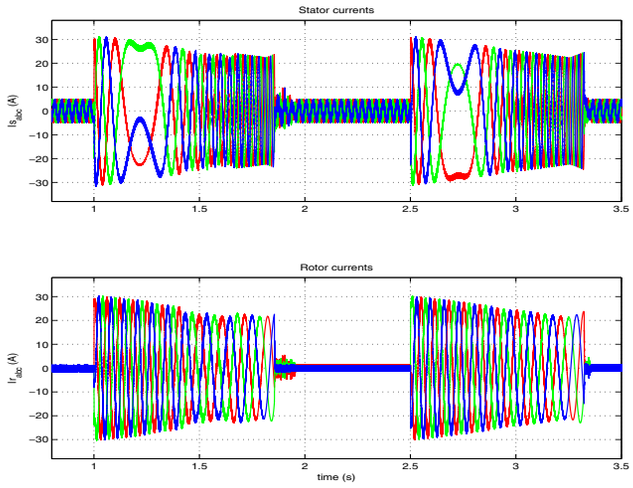

Figure 13. Stator and rotor current for speed reversion for DTC-SVM with PI-F controller.

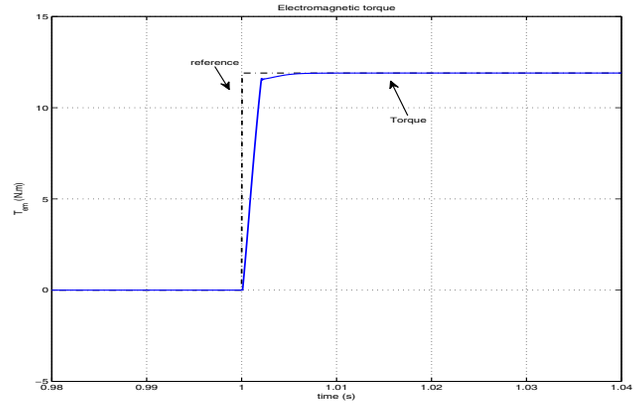

Figure 14. Sudden torque change for DTC-SVM whit PI-F controller

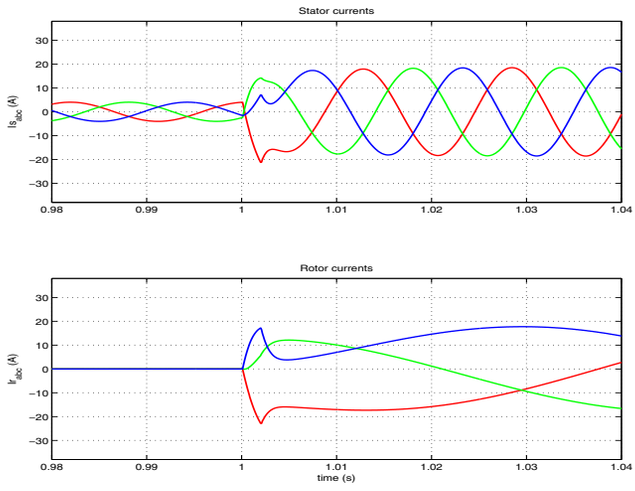

Figure 15. Stator and rotor currents for sudden torque change for DTC-SVM with PI-F controller.

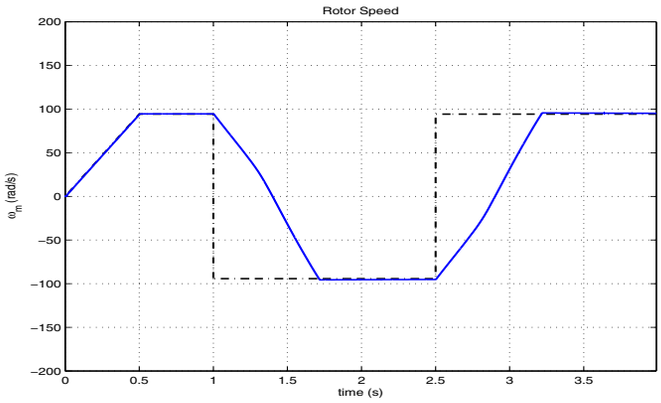

Figure 16. Speed reversion for DTC-SVM with PIF controller.

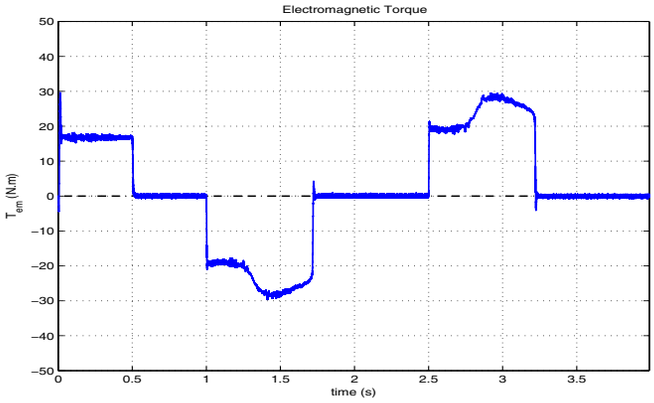

Figure 17. Torque bahavior for speed reversion for DTC-SVM with PIF controller.

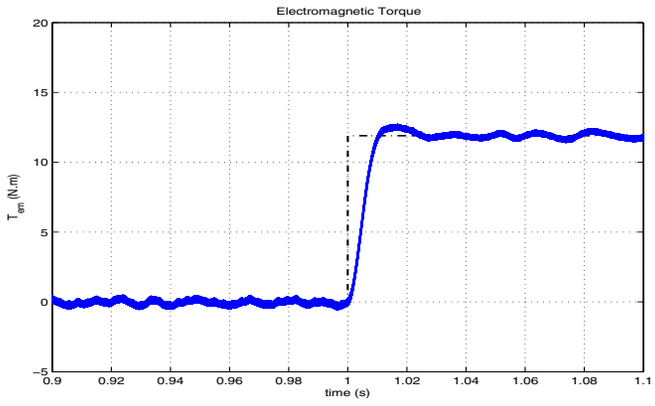

Figure 18. Sudden torque change for DTC-SVM whit PIF controller.

Fig. 21 presents the results when a specific torque profile is imposed to DTC-SVM scheme with STPIF controller. In this case the electromagnetic torque follow the reference.

Fig. 22 illustrates the response of the electromagnetic torque for the DTC-SVM scheme with STPIF controller, when applying step change in the motor load. In this test we used the rise time $t_r = 5.49mS$, the settling time $t_s = 12mS$ and the integral-of-time multiplied by the absolute magnitude of the error index $ITAE = 199.5$.

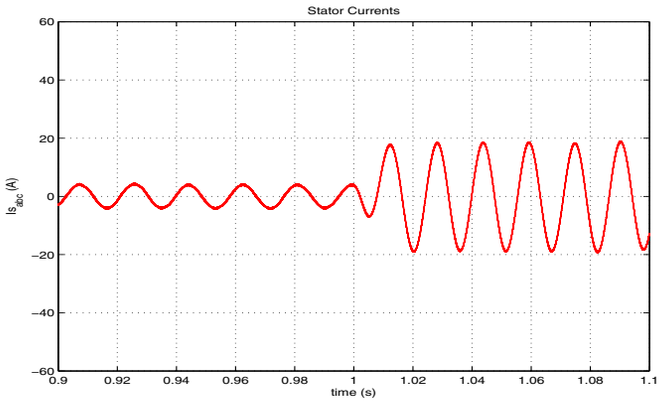

Figure 19. Phase *a* stator current for sudden torque change for DTC-SVM with PIF controller.

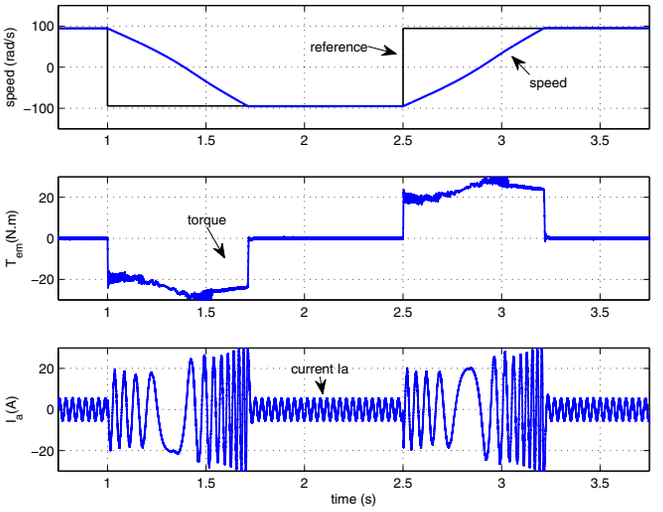

Figure 20. Speed, torque and phase *a* stator current for speed reversion for DTC-SVM with STPIF controller.

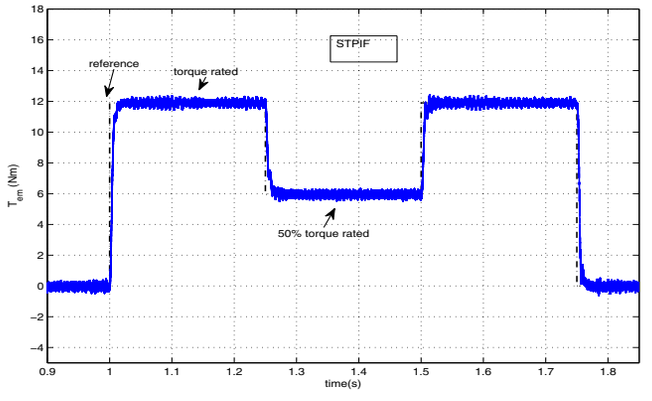

Figure 21. Torque profile for DTC-SVM whit STPIF

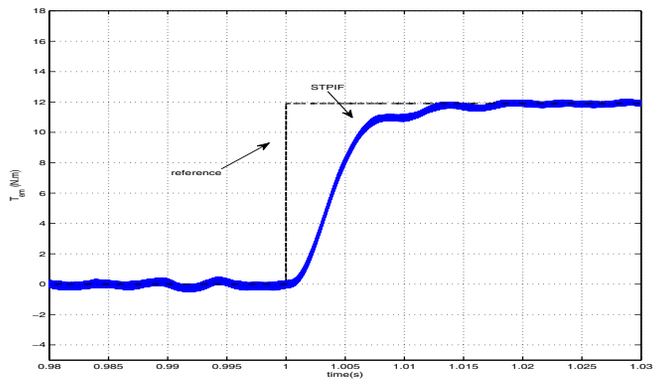

Figure 22. Step change in torque for DTC-SVM scheme with STPIF

Rated voltage (V)	220/60Hz
Rated Power (W)	2238
Rated Torque (Nm)	11.9
Rated Speed (rad/s)	179
$R_s, R_r (\Omega)$	0.435, 0.816
L_{ls}, L_{lr} (H)	0.002, 0.002
L_m (H)	0.0693
$J(K_g m^2)$	0.089
P	2

Table 5. Induction Motor Parameters [12]

6. Conclusion

In this chapter we have presented the DTC-SVM scheme that controls a three-phase IM using three different kinds of fuzzy controllers. These fuzzy controllers were used in order to determinate dynamically and on-line the load angle between stator and rotor flux vectors. Therefore, we determine the electromagnetic torque necessary to supply the motor load. We have conducted simulations with different operating conditions. Our simulation results show that the all proposed fuzzy controllers work appropriately and according to the schemes reported in the literature. However, the STPIF controller achieves a fast torque response and low torque ripple in a wide range of operating conditions such as: sudden change in the command speed and step change of the load.

Acknowledgements

The authors are grateful to FAPESP and CAPES for partially financial support.

Author details

José Luis Azcue and Ernesto Ruppert
School of Electrical and Computer Engineering of University of Campinas, UNICAMP, Department of Energy Control and Systems, Campinas-SP, Brazil

Alfeu J. Sguarezi Filho
CECS/UFABC, Santo André - SP, Brazil

7. References

[1] Abu-Rub, H., Guzinski, J., Krzeminski, Z. & Toliyat, H. [2004]. Advanced control of induction motor based on load angle estimation, *Industrial Electronics, IEEE Transactions on* 51(1): 5 – 14.

[2] Azcue P., J. L. [2010]. *Three-phase induction motor direct torque control using self-tuning pi type fuzzy controller*, Master's thesis, University of Campinas (UNICAMP).

[3] Azcue P., J. & Ruppert, E. [2010]. Three-phase induction motor dtc-svm scheme with self-tuning pi-type fuzzy controller, *Fuzzy Systems and Knowledge Discovery (FSKD), 2010 Seventh International Conference on*, Vol. 2, pp. 757 –762.

[4] Bertoluzzo, M., Buja, G. & Menis, R. [2007]. A direct torque control scheme for induction motor drives using the current model flux estimation, *Diagnostics for Electric Machines, Power Electronics and Drives, 2007. SDEMPED 2007. IEEE International Symposium on* pp. 185 –190.

[5] Cao, S.-G., Rees, N. & Feng, G. [1999]. Analysis and design of fuzzy control systems using dynamic fuzzy-state space models, *Fuzzy Systems, IEEE Transactions on* 7(2): 192 –200.

[6] Chen, C.-L. & Chang, M.-H. [1998]. Optimal design of fuzzy sliding-mode control: A comparative study, *Fuzzy Sets and Systems* 93(1): 37 – 48.
URL: *http://www.sciencedirect.com/science/article/pii/S0165011496002217*

[7] Chen, S., Kai, T., Tsuji, M., Hamasaki, S. & Yamada, E. [2005]. Improvement of dynamic characteristic for sensorless vector-controlled induction motor system with adaptive pi mechanism, *Electrical Machines and Systems, 2005. ICEMS 2005. Proceedings of the Eighth International Conference on*, Vol. 3, pp. 1877 –1881 Vol. 3.

[8] Depenbrock, M. [1988]. Direct self-control (dsc) of inverter-fed induction machine, *Power Electronics, IEEE Transactions on* 3(4): 420–429.

[9] Habetler, T., Profumo, F., Pastorelli, M. & Tolbert, L. [1992]. Direct torque control of induction machines using space vector modulation, *Industry Applications, IEEE Transactions on* 28(5): 1045 –1053.

[10] Koutsogiannis, Z., Adamidis, G. & Fyntanakis, A. [2007]. Direct torque control using space vector modulation and dynamic performance of the drive, via a fuzzy logic controller for speed regulation, *Power Electronics and Applications, 2007 European Conference on* pp. 1 –10.

[11] Kovacic, Z. & Bogdan, S. [2006]. *Fuzzy Controller Design: Theory and Applications*, CRC Press.

[12] Krause, P. C., Wasynczuk, O. & Sudhoff, S. D. [2002]. *Analysis of Electric Machinery and Drive Systems*, IEEE Press.

[13] Lascu, C., Boldea, I. & Blaabjerg, F. [2000]. A modified direct torque control for induction motor sensorless drive, *Industry Applications, IEEE Transactions on* 36(1): 122–130.

[14] Rodriguez, J., Pontt, J., Silva, C., Kouro, S. & Miranda, H. [2004]. A novel direct torque control scheme for induction machines with space vector modulation, *Power Electronics Specialists Conference, 2004. PESC 04. 2004 IEEE 35th Annual*, Vol. 2, pp. 1392 – 1397 Vol.2.

[15] Takahashi, I. & Noguchi, T. [1986]. A new quick-response and high-efficiency control strategy of an induction motor, *Industry Applications, IEEE Transactions on* IA-22(5): 820 –827.
[16] Trzynadlowski, A. M. [1993]. *The Field Orientation Principle in Control of Induction Motors*, springer.
[17] Vas, P. [1998]. *Sensorless Vector and Direct Torque Control*, Oxford University Press. ISBN 0198564651.
[18] Viola, J., Restrepo, J., Guzman, V. & Gimenez, M. [2006]. Direct torque control of induction motors using a fuzzy inference system for reduced ripple torque and current limitation, *Power Electronics and Motion Control Conference, 2006. EPE-PEMC 2006. 12th International*, pp. 1161 –1166.
[19] Yamakawa, T. [1993]. A fuzzy inference engine in nonlinear analog mode and its application to a fuzzy logic control, *Neural Networks, IEEE Transactions on* 4(3): 496 –522.